

International Journal of Scientific Research and Reviews

Detection of Trap Energy Levels in Thermally Evaporated 3,5-Bis(4-Tert-Butylphenyl)-4-Phenyl-4h-1,2,4-Triazole Thin Films by Temperature Dependent Admittance Spectroscopy

Gurpreet Singh^{1*} and Ramanpreet Kaur Aulakh²

Guru Nanak Dev University College, Narot Jaimal Singh, Pathankot, Punjab, India-145026.

Guru Nanak Dev University College, Patti, Tarn-Taran Sahib, Punjab, India-143416.

ABSTRACT

Performance of multilayered optoelectronic devices is strongly dependent upon accurate energy band structure at the interfaces. The presence of trap centers and other defects is a common feature of these types of multilayered devices which limits the performance due to recombinations of charge carriers. The organic material 3,5-Bis(4-tert-butylphenyl)-4-phenyl-4H-1,2,4-triazole (abbreviated as BBPT) is studied to determine trap energy levels to best judge its energy band structure in multilayered devices. Temperature dependent admittance spectroscopy is used to characterize ITO/3,5-Bis(4-tert-butylphenyl)-4-phenyl-4H-1,2,4-triazole/Al device configuration to determine the trap energy levels. It is further confirmed by estimating the Urbach's energy from UV-Visible absorption spectroscopy of the BBPT thin film. Estimation of trap centers will be beneficial for use of BBPT as a carrier transport layer in optoelectronic devices.

KEYWORDS: Admittance, defects, multilayered, optoelectronic, recombination, spectroscopy.

***Corresponding author**

Gurpreet Singh

Gurpreet Singh

Assistant Professor, Department of Physics

Guru Nanak Dev University College,

Narot Jaimal Singh, Pathankot-145026, India.

M: +91-8288018439, E-Mail: gsjosan.phy@gmail.com

INTRODUCTION

Multilayered Optoelectronic devices such as Organic light emitting diodes (OLEDs) and Organic Photovoltaic cells (OPVCs) have attracted much attention since last two decades, to meet with the increasing energy demand at low cost¹⁻⁴. The uninterrupted flow of charge carriers between cathode and anode can be achieved by minimizing the interface barrier, which can enhance the performance of these devices. It can be achieved by insertion of carrier transport layers such as electron transport layer (ETL) and hole transport layer (HTL) in between the emissive/absorbing layer and electrodes^{3,5}. The technology and efficiency of these devices is matured to such an extent by the introduction of carrier transport layers, that these optoelectronic devices are now being used commercially at a large scale to fabricate flat panel displays and solar panels⁶.

In this communication, the material under investigation 3,5-Bis(4-tert-butylphenyl)-4-phenyl-4H-1,2,4-triazole (abbreviated as BBPT) is a transparent, conducting material with high band gap and amorphous morphology in thin film configuration. These are ideal characteristics for a material to be used as a carrier transport layer in optoelectronic devices⁵. However, for its possible use as an electron transporting material in optoelectronic devices, it is required to understand its accurate energy band formation with electrodes by determining the trap energy levels and other defects at the interfaces. It is because the performance of these devices is strongly dependent upon interface recombinations of charge carriers at trap energy levels and other structural defects. These trap levels or defects are commonly present in large area amorphous morphology of thin films in the multilayered structure⁷.

Various techniques like deep-level transient spectroscopy (DLTS)⁸, photoconductivity (PC)⁹, modulated photocurrent (MPC)¹⁰, time of flight (TOF)¹¹ etc. have been used to identify these defect distributions. However, temperature dependent admittance spectroscopy is a simple and highly accurate technique to determine recombination parameters for a trap energy state^{7,12-15}. To find the trap energy levels in BBPT an ITO/BBPT/Al device is fabricated and characterized for temperature dependent admittance spectroscopy.

EXPERIMENTAL

The compound 3,5-Bis(4-tert-butylphenyl)-4-phenyl-4H-1,2,4-triazole (BBPT) is purchased from Sigma Aldrich Corporation. Thin film of BBPT is deposited on chemically and ultrasonically cleaned ITO substrate by thermal evaporation using Hind High Vacuum 12A4D vacuum coating unit, followed by deposition of Al to fabricate ITO/BBPT/Al device. Evaporation of the materials is done at base pressure of 2×10^{-5} Torr using a tungsten boat by keeping the evaporation rate constant at

9 Å/s. BBPT film is also deposited on quartz substrate by following the similar procedure. Surface morphology of thin film deposited on ITO substrate is studied using atomic force microscope (AFM) (Nanosurf easyscan2, Switzerland) in tapping mode by scanning an area of $4.92\mu\text{m} \times 4.92\mu\text{m}$. UV-visible spectrum of film was studied using Shimadzu Spectrophotometer UV 2450. The ITO/BBPT/Al device is characterized for temperature dependent admittance spectroscopy and other frequency dependent characteristics using HIOKI 3522 and 3532 LCR hightester.

RESULTS AND DISCUSSION

Surface morphology is an important parameter to determine the quality of thin film of an organic material. Figure 1, shows AFM image of BBPT thin film deposited on ITO substrate by thermal evaporation.

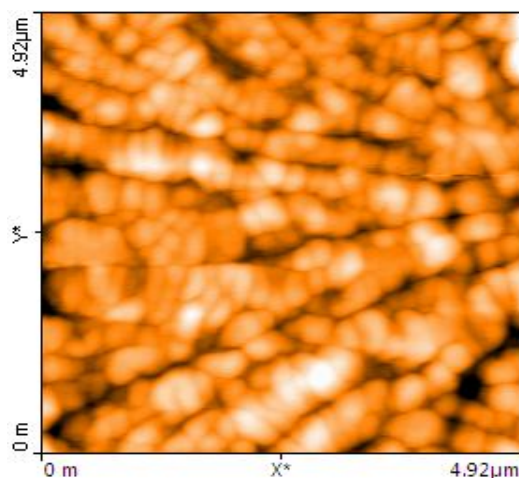


Figure 1 AFM image of BBPT thin film prepared on ITO substrate

Uniform and crack-free growth of film is confirmed with observed root mean squared (RMS) surface roughness of 17 nm. Small size grains having average base width of 180 nm are observed to form randomly distributed chains with length 3-4 μm . the long chains will be beneficial for charge transport. This study reveals a fine growth of thin film over ITO substrate.

The ac Conductance (G) and Capacitance (C) of the ITO/BBPT/Al device are measured in the temperature range 80K to 350 K and frequency range from 500Hz to 4 kHz. Variation of ac conductance and capacitance with temperature for various frequencies is shown in figure 2, and figure 3, respectively.

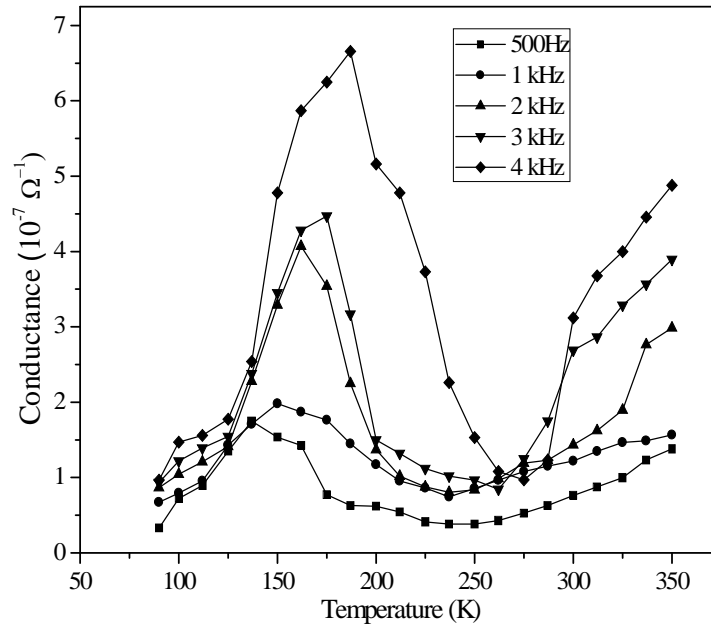


Figure 2: Variation of ac conductance with temperature for various frequencies

It is observed that ac conductance increases with increase in temperature at a fixed frequency, reaches a maximum and then decreases with increase in temperature. This variation is in accordance with the theory of conductance and capacitance of a metal/semiconductor Schottky barrier in the presence of trap levels¹²⁻²¹. The variation of ac conductance with respect to various parameters is governed by the equation:

$$G_c = \frac{e_n \omega^2 N_t}{e_n^2 + \omega^2 n} A \left(\frac{q \epsilon N_+}{2V_D + 2V_R} \right)^{1/2} \quad (1)$$

Where ω = Angular frequency of applied ac signal, e_n is the emission rate of trap, n is free electron concentration in bulk, N_t and N_+ are trap density and fixed-charge density in depletion region respectively, A is area of the device, V_D is barrier height, V_R is reverse bias voltage and ϵ is the permittivity of the material.

The emission rate e_n is a function of temperature, which is expressed as¹⁵⁻¹⁶:

$$e_n = e_{n0} \exp\left(-\frac{E_t}{kT}\right) = C_n N_c \exp\left(-\frac{E_t}{kT}\right) \quad (2)$$

Here, V_{th} is the thermal velocity of the carrier, $C_n = \sigma_n V_{th}$ is the capture coefficient, σ_n is the capture cross section, E_t is the trap energy level below the conduction band edge and N_c is the density of states in conduction band. The above expression shows that emission rate e_n is dependent upon temperature and hence the ac conductance. At a temperature (T_p) where emission rate of trap level equates the angular frequency (ω) of applied ac signal, the conductance reaches its maximum value. This peak in the conductance vs temperature curve represents a trap level existing near the

conduction band of BBPT. It is observed that with increase in frequency of the applied signal, the peak in the G-T curve shifts towards higher temperature, which is obvious trend in the admittance spectroscopy¹⁵.

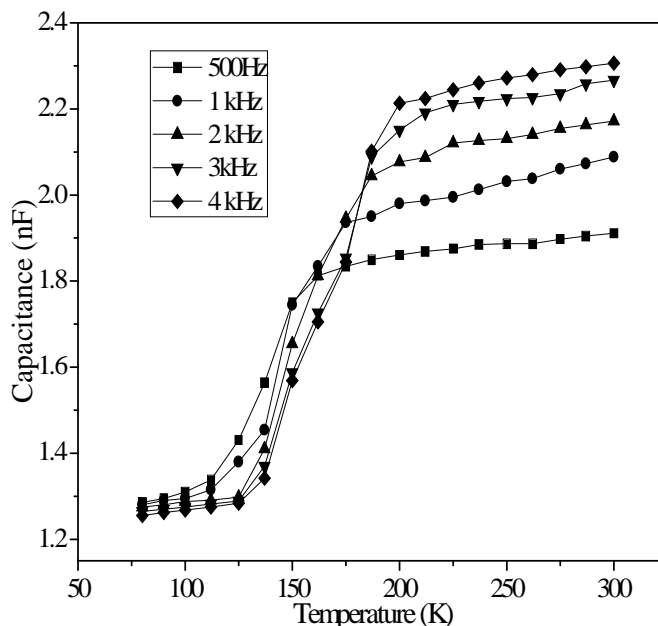


Figure 3: Variation of Capacitance of ITO/BBPT/Al device with temperature

The study of Capacitance of ITO/BBPT/Al device with temperature shows that capacitance is strongly dependent on temperature. The variation of capacitance is governed by the equation¹⁵⁻¹⁶:

$$C_r = \frac{\epsilon_n}{\epsilon_n^2 + \omega^2} \frac{N_t}{n} A \left(\frac{q\epsilon N_+}{2V_D + 2V_R} \right)^{1/2} \quad (3)$$

Corresponding to every peak in the conductance vs temperature curve studied at different frequencies, an inflection point is observed in each capacitance vs temperature curve of Figure 3. It is in close agreement with the theory of trap energy levels and confirms the presence of trap level in BBPT.

From Equation (2), it is clear that when $\epsilon_n = \omega$ at temperature T_p (Temperature at which rate of emission from the trap energy level equates the angular frequency of the applied signal) a graph between natural logarithm of ω/T_p^2 vs $1000/T_p$ will be a straight line. Figure 4, shows similar results. The trap energy calculated from the slope of this graph is 0.707 eV.

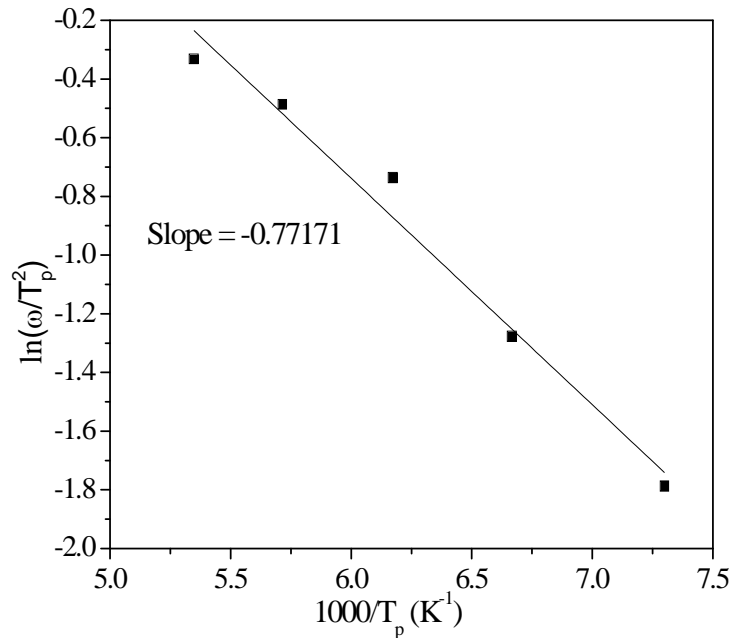


Figure 4: Variation of $\ln(\omega/\Gamma_p^2)$ vs $1000/T_p$

Presence of trap energy levels may further be confirmed by finding the Urbach's energy. Urbach energy can be calculated from the Urbach tail which is an exponential part of the Optical absorption coefficient curve in the lower absorption edge. This exponential tail appears in disordered or amorphous materials due to presence of localized states extended in the band gap. In the optical region near the absorption edge, the absorption coefficient obeys an empirical relation known as Urbach's rule²²⁻²⁵ given by:

$$\alpha = \alpha_0 \exp(h\nu/E_U) \quad (4)$$

Where α is the optical absorption coefficient of BBPT thin film, h is Planck's constant, ν is the frequency of incident UV-Visible radiation and E_U is the Urbach's energy. The further investigation and confirmation of trap energy levels or energetic disorders, is studied using non-transport method, i.e. UV-Visible absorption spectroscopy. Figure 5, shows the UV-Visible absorption spectrum of BBPT thin film Studied at room temperature in the wavelength range 200-600 nm.

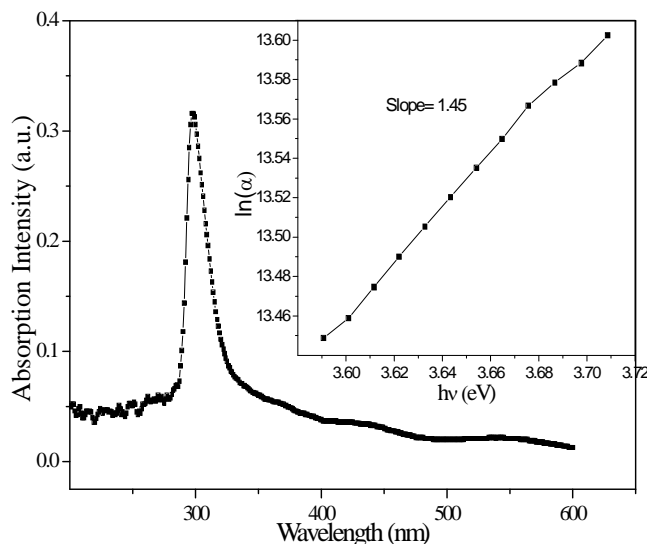


Figure 5: UV-Visible absorption spectrum of BBPT film prepared by thermal evaporation and Variation of $\ln(\alpha)$ vs incident photon energy ($h\nu$) (inset)

Strong absorption peak is observed in the UV region from 290 nm to 330 nm with maximum absorption at 297 nm which shows that it is transparent for visible light, which make it suitable material to be used as a carrier transport layer in optoelectronic devices. Figure 5 (inset), shows the variation of $\ln(\alpha)$ vs incident photon energy ($h\nu$). Urbach's energy E_U is calculated from inverse of the slope of graph between $\ln(\alpha)$ and incident photon energy ($h\nu$) which is found to be 0.689 eV. This value of Urbach's energy is in close agreement with Trap energy levels calculated from admittance spectroscopy. These results confirm the existence of trap levels near the conduction band edge of BBPT.

CONCLUSION

Organic material 3,5- Bis(4-tert-butylphenyl)-4-phenyl-4H-1,2,4-triazole (BBPT) is studied for temperature dependent admittance spectroscopy in ITO/BBPT/Al configuration to determine trap energy levels. A peak in the plot of conductance vs. temperature is observed at a temperature (T_p) where emission rate of trap level equates the angular frequency (ω) of applied ac signal. Corresponding to every peak in the conductance vs. temperature plot an inflexion point is observed in capacitance vs. temperature plot of ITO/BBPT/Al device. These results are in good correlation with theory of trap energy levels and confirm the presence of trap level in BBPT. For better understanding of energy band structure at the junction of BBPT with any suitable material for an optoelectronic device, the trap energy (0.707 eV) is calculated which is further confirmed by finding the Urbach's energy from optical absorption coefficient curve in the lower absorption edge. The

knowledge of trap energy level will be a key factor to find best suitable materials to fabricate an efficient multilayered optoelectronic device using BBPT as a carrier transport layer.

ACKNOWLEDGMENT

The authors would like to acknowledge Material Science Research Lab, Department of Physics, Guru Nanak Dev University, Amritsar, for providing the necessary equipment and facilities to carry out this work.

REFERENCES

1. Lee JH, Wang PS, Park HD, Wu CI and Kim JJ. A high performance inverted organic light emitting diode using an electron transporting material with low energy barrier for electron injection. *Organic Electronics*.2011; 12(11): 1763-1767.
2. Pfeiffer M, Forrest SR, Zhou X and Leo K. A low drive voltage, transparent, metal-free n-i-p electrophosphorescent light emitting diode. *Organic Electronics*. 2003; 4(1):21-26.
3. Petritsch DIK. Organic Solar Cell Architectures. PhD Thesis, University of Cambridge, United Kingdom and Technische Universität Graz, Austria. 2000.
4. Uddin MA, Chan HP and Rahman BMA. Structural improvement of organic photovoltaic cell (opvc) towards higher efficiency. *Reviews on advanced material science*.2010;26: 58-66.
5. Kulkarni AP, Tonzola CJ, Babel A and Jenekhe SA. Electron Transport Materials for Organic Light-Emitting Diodes. *Chemistry of materials*.2004; 16(23): 4556-4573.
6. Some company websites:<https://www.oled-info.com/lg-officially-launches-its-oled-wallpaper-commercial-display>,<https://www.lg.com/us/business/commercial-display>,<http://www.noritake-iron.jp/eng/products/oled/index.html>.
7. Burgelman M and Nollet P. Admittance spectroscopy of thin film solar cells. *Solid state ionics*, 2005; 176 (25-28): 2171-2176.
8. Lang DV, Grimmeiss HG, Meijer E and Jaros M. Complex nature of gold-related deep levels in silicon. *Physical Review B*. 1980; 22(8): 3917-3934.
9. Rose R. Book titled: Concepts in Photoconductivity. Interscience: New York; 1963.
10. Oheda H. Phaseshift analysis of modulated photocurrent: Its application to the determination of the energetic distribution of gap states. *Journal of Applied Physics*. 1981;52(11): 6693-6700.
11. LeComber PG and Spear WE. Electronic transport in amorphous silicon films. *Physical Review Letters*. 1970;25(8): 509-511.

12. Losse DL. Admittance spectroscopy of impurity levels in Schottky barriers. *Journal of Applied Physics*. 1975; 46(5): 2204-2214.
13. Vincent G, Bois D and Pinard P. Conductance and capacitance studies in Gap Schottky barriers. *Journal of Applied Physics*. 1975; 46(12):5173-5178.
14. Vincent KG. Spectroscopy of traps in GaAlAs light emitting diodes. *Solid State Communication*. 1976;19(6): 559-561.
15. Yousuf M, Kuliyeve B and Lalevic B. Investigation of trapping centers in single-crystal niobium dioxide by admittance spectroscopy. *Journal of Applied Physics*. 1982;53(12): 8647-8652.
16. Shockley W and Read WT. Statistics of the Recombinations of Holes and electrons. *Journal of Physical Review*. 1952; 87(5): 835-842.
17. Chen JF, Chen NC and Liu HS. Characterizations of deep levels in SnTe-doped GaSb by admittance spectroscopy. *Applied Physics Letters*. 1996;69(13): 1891-1893.
18. Xu JH and Shen J. Effects of discrete trap levels on carrier transport in organic electroluminescent devices. *Journal of Applied Physics*. 1998; 83(5): 2646-2648.
19. Djebbour Z, Darga A and Dubois AM et al. Admittance spectroscopy of cadmium free CIGS solar cells heterointerfaces. *Thin Solid Films*. 2006; 511: 320–324.
20. Marin AT, Musselman KP and MacManus-Driscoll JL. Accurate determination of interface trap state parameters by admittance spectroscopy in the presence of a Schottky barrier contact: Application to ZnO-based solar cells. *Journal of Applied Physics*. 2013;113(14): 144502-144510.
21. Kaya A, Sevgili O and Altindal S. Energy density distribution profiles of surface states, relaxation time and capture cross-section in Au/n-type 4H-SiC SBDs by using admittance spectroscopy method. *International Journal of Modern Physics B*. 2014; 28(17): 1450104-1450116.
22. Singh S and Prasher S. A comparison of modifications induced by Li^{3+} and O^{6+} ion beam to Makrofol-KG and CR-39 polymeric track detectors. *Nuclear Instruments and Methods in Physics Research Section B*. 2006;244(1): 252–256.
23. Neerja, Kalia S, Kaur J, Kumar S and Singh S. The Optical and Chemical Response of Thermal Neutron-Irradiated CR-39 Polymeric Track Detector after Annealing. *Polymer-Plastics Technology and Engineering*. 2014;53: 526–530.
24. Robertson J and Reilly EPO. Electronic and atomic structure of amorphous carbon. *Physical Review B*. 1987;35(6): 2946–2957.
25. Singh L and Samra KS. Surface and Bulk Structure Characterization of Proton (3 MeV) Irradiated Polycarbonate, *Journal of Macromolecular Science Part B*. 2007;46(5): 1041–1049.